

(1)

Spatially Resolved Tunneling Spectroscopy & Spin-Polarized Quasiparticle Transport in Cuprate Superconductors

NAI-CHANG YEH
Department of Physics, California Institute of Technology

1. Introduction

- Doped Mott insulators & competing orders**
- Unconventional pairing symmetry & mechanism**

2. Quasiparticle Tunneling Spectroscopy

- Quasiparticle transport at N/S interface**
- Generalized BTK theory**
- Comparison of planar & STM junctions**
- Directional & spatially resolved tunneling spectroscopy of cuprate superconductors**
- Effects of impurities**

3. Spin-Polarized Quasiparticle Transport

- Magnetic pair-breaking effects**
- Conventional nonequilibrium superconductivity**
- Suppression of high-temperature superconductivity by spin injection**
- Implication of the microscopic mechanism**

(2)

In collaboration with :

- C.-C. Fu (Physics, Caltech)**
- C.-T. Chen (Physics, Caltech)**
- Z. Huang (Physics, Caltech)**
- Dr. R. P. Vasquez (JPL, Caltech)**
- Dr. S. Tajima (SRL, Japan)**
- Prof. X.-X. Xi (Penn. State Univ.)**
- Dr. W.-D. Si (Penn. State Univ.)**

Acknowledgement :

- NSF/DMR**
- NASA/OSS**

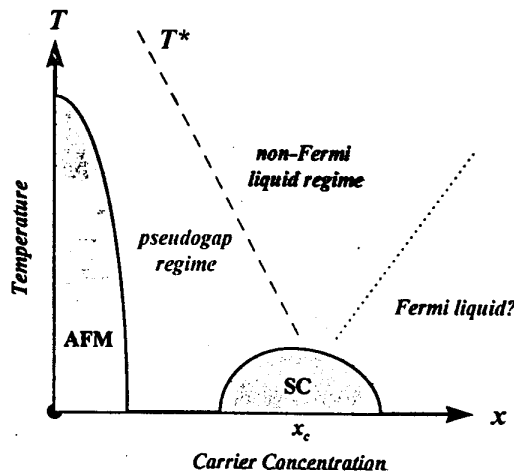
Yeh
Seminar 2

(3)

1. Introduction

A. Doped Mott Insulators & Competing Orders

- Mott insulators: conduction blocked by e-e repulsion.
(conventional band insulators: conduction blocked by Pauli exclusion principle)
- High-temperature superconductors are doped Mott insulators.
- Quasi-2D & proximity to a Mott insulating phase
→ unconventional normal-state properties.
- Relevance of a quantum critical point (x_c)?



• Global Symmetries in Doped Antiferromagnetic Square Lattice:

- * S -- the electromagnetic $U(1)$ symmetry;
(broken by the appearance of superconducting order)
- * M -- the $SU(2)$ spin rotation invariance symmetry;
(broken by the appearance of magnetic order)
- * C -- the space group of the square lattice (including parity P);
(broken by charge/spin density inhomogeneity)
- * T -- time reversal symmetry;

• Competing Orders that Break "S", "C" and/or "T" Symmetries:

- * $d_{x^2-y^2}$ -- $U(1)$ broken symmetry;
 - * $(d_{x^2-y^2} + id_{xy})$ -- $U(1)$, P, T broken symmetries & PT conserved;
 - * $(d_{x^2-y^2} + is)$ -- $U(1)$ and T broken symmetries;
 - * Wigner crystals -- $U(1)$ and "C" broken symmetries;
 - * Wigner crystals of hole pairs -- $U(1)$ and "C" broken symmetries;
 - * Orbital antiferromagnets -- $U(1)$, T, "C" broken symmetries;
 - * Stripe phase -- $U(1)$ & "C" broken symmetries;
 - * Circulating current phase -- $U(1)$ & "T" broken symmetries.
- ↔ Relevance of doping level, disorder & thermal fluctuations.

(4)

(5)

B. Unconventional Pairing Symmetry & Mechanism

- Predominantly $d_{x^2-y^2}$ pairing symmetry in all cuprate superconductors.

[Tsuei et al. (1994); van Harlingen (1995); Wei et al. (1998); Alff et al. (1998); Kirtley et al. (1999); Yeh et al. (2000)]

→ anisotropic superconducting gap & low-energy excitations.

- Possibilities of secondary pairing components:

* Anyon superconductivity $\leftrightarrow (d_{x^2-y^2}+id_{xy})$ pairing.

* Doppler effect on quasiparticle spectra at {110} surfaces
 $\rightarrow (d_{x^2-y^2}+is)$.

- Existence of spin-charge separation:

* Independent spectra of excitations for charge and for spin.

* Non-Fermi liquid behavior in the normal state.

\leftrightarrow Resonating Valence bond (RVB) scenario? (spinons & holons)

\leftrightarrow Stripe-phase scenario, Luttinger liquid?

- Our experimental investigation:

* Scanning tunneling spectroscopy (STS),

→ pairing potential, pseudogap, pairing symmetry.

* Spin-injection & nonequilibrium effects,

→ spin & charge transport characteristics.

* Experimental signatures:

Test	$d_{x^2-y^2}$	$(d_{x^2-y^2}+id_{xy})$	$(d_{x^2-y^2}+is)$
<u>Splitting in ZBCP?</u>	no	yes	yes
<u>Quasiparticle bound states in vortex cores?</u>	no	yes	yes
<u>Local DOS at non-magnetic impurities?</u>	one peak at energy Ω	two peaks at energies $\pm \Omega$	two peaks at energies $\pm \Omega$
<u>Total flux at a π-junction?</u>	π -GBJ: $0.5\Phi_0$ (JJ: Φ_0)	$< 0.5\Phi_0$	$< 0.5\Phi_0$

* Recent development:

- Evidence of non-magnetic impurity-stabilized $(d_{x^2-y^2}+id_{xy})$ pairing from scanning SQUID microscopy:

-- spontaneous magnetization with random signs and total flux $\Phi < 0.5\Phi_0$ on impurity sites (Y_2O_3 , Y_2BaCuO_5 , etc.)
[Tafuri & Kirtley, cond-mat/0003106]

- $Sp(2N)$ t-J model in the large-N limit for competing orders and quantum criticality in doped antiferromagnets:

-- possibility of ground state $d_{x^2-y^2}$ with near by $(d_{x^2-y^2}+id_{xy})$ or $(d_{x^2-y^2}+is)$ states. [Vojta, Zhang, and Sachdev, cond-mat/0003163]

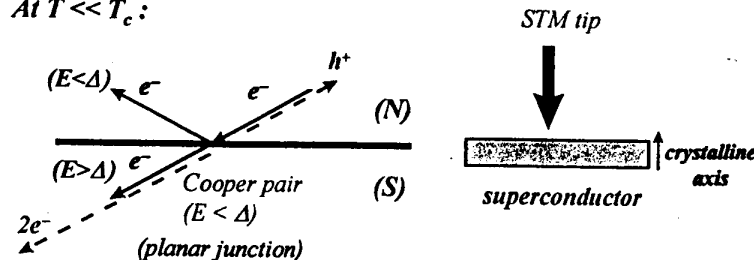
(6)

2. Quasiparticle Tunneling Spectroscopy

A. Quasiparticle transport at N/S interfaces

(N: normal metal; S: superconductor)

At $T \ll T_c$:



■ High-barrier tunnel junctions [large Z] ($Z \sim \frac{\text{barrier height}}{\text{Fermi energy}}$)

- * $E > \Delta$: transmission of electron-like quasiparticles over a charge diffusion length Λ_Q . (E : quasiparticle energy)

- * $E < \Delta$: complete normal reflection.

■ Low-barrier point-contact junctions [small Z]

- * $E > \Delta$: transmission of electron-like quasiparticles over Λ_Q .

- * $E < \Delta$: reflection of holes and transmission of Cooper pairs.

→ Andreev reflection (with enhancement of conductance).

■ General N/S interface [arbitrary Z]

- * **Normal and Andreev reflections.**

BTK theory: Blonder, Tinkham and Klapwijk,
Phys. Rev. B 25, 4515 (1982).

(7)

(8)

Generalized BTK Theory

[Hu, Tanaka & Kashiwaya, (1994)]

SIN tunneling current: (for superconducting gap function Δ_k)

$$I_{NS} = G_0 \mu_B \int e^{-(k_F/\beta)^2 d^2 k_F} \int dE_k [1 + A(E_k, \Delta_k, Z) - B(E_k, \Delta_k, Z)] / [f(E_k - eV) - f(E_k)]$$

\downarrow Andreev reflection

$$\left\{ \begin{array}{l} Z = \frac{2\pi mH}{\hbar^2 k_F} = \text{barrier strength} \\ f(E_k) = \text{Fermi function} = \frac{1}{1 + \exp(E_k/(k_B T))} \end{array} \right.$$

\downarrow normal reflection

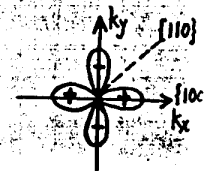
$$\beta = \text{tunneling cone}$$

$$E_k = \text{quasiparticle energy} = \sqrt{\xi_k^2 + \Delta_k^2}$$

\downarrow transverse k -vector

$$= \text{normal state tight-binding energy relative to } E_F$$

$$= -2t[\cos(k_x a) + \gamma \cos(k_y a)] + 4t'[\cos(k_x a) \cos(k_y a)]$$



$$(1 + A - B) = \left\{ \frac{16(1 + |\Gamma_\pm|^2) \cos^4 \theta_k + 4Z^2(1 - |\Gamma_\pm|^2) \cos^2 \theta_k}{4 \cos^2 \theta_k + Z^2[1 - \Gamma_\pm \exp(i\varphi_k - i\varphi_\pm)]^2} \right\}$$

$$\Gamma_\pm = (E_k / |\Delta_{k,\pm}|) - \sqrt{(E_k / |\Delta_{k,\pm}|)^2 - 1} \quad \exp(i\varphi_\pm) = \Delta_{k,\pm} / |\Delta_{k,\pm}|$$

$d_{x^2-y^2}$ gap function: $\Delta_k = \Delta_d [\cos(k_x a) - \cos(k_y a)] \approx \Delta_d \cos(2\theta_k)$

Mixed symmetries:

$$\left\{ \begin{array}{l} (d_{x^2-y^2} + is) : \Delta_k = \Delta_d \cos(2\theta_k) + i\Delta_s \\ (d_{x^2-y^2} + id_{xy}) : \Delta_k = \Delta_d \cos(2\theta_k) + i\Delta'_d \sin(2\theta_k) \end{array} \right.$$

(9)

C. Comparison of Scanning Tunneling Spectroscopy (STS) & Planar Junctions

	STS	Planar Junctions
<i>Junction Area</i>	$10^{-8} \sim 10^{-5} \mu\text{m}^2$	$10^2 \sim 10^5 \mu\text{m}^2$
<i>Tunnel Currents</i>	$10^{-7} \sim 10^{-6} \text{ mA}$	$10^0 \sim 10^2 \text{ mA}$
<i>Voltage Resolution</i>	$10^{-2} \sim 10^0 \text{ mV}$	$10^{-4} \sim 10^{-3} \text{ mV}$
<i>Voltage Range</i>	$>\sim 10^2 \text{ mV}$	$\sim 10^1 \text{ mV}$
<i>Insulating Barrier</i>	(vacuum gap)	(deposited layers of insulators)
<i>Probing Depth</i>	surface ($< 10^2 \text{ nm}$)	bulk

* Thermal smearing: At $T = 10.0 \text{ K}$, $\delta V < \sim 10^0 \text{ mV}$
 $T = 1.0 \text{ K}$, $\delta V < \sim 10^{-1} \text{ mV}$
 $T = 0.1 \text{ K}$, $\delta V < \sim 10^{-2} \text{ mV}$

↔ Voltage resolution must be smaller than the thermal smearing to be relevant.

(10)

D. Directional & Spatially Resolved Tunneling Spectroscopy Studies of Superconducting Cuprates

■ **Samples for STS studies:**

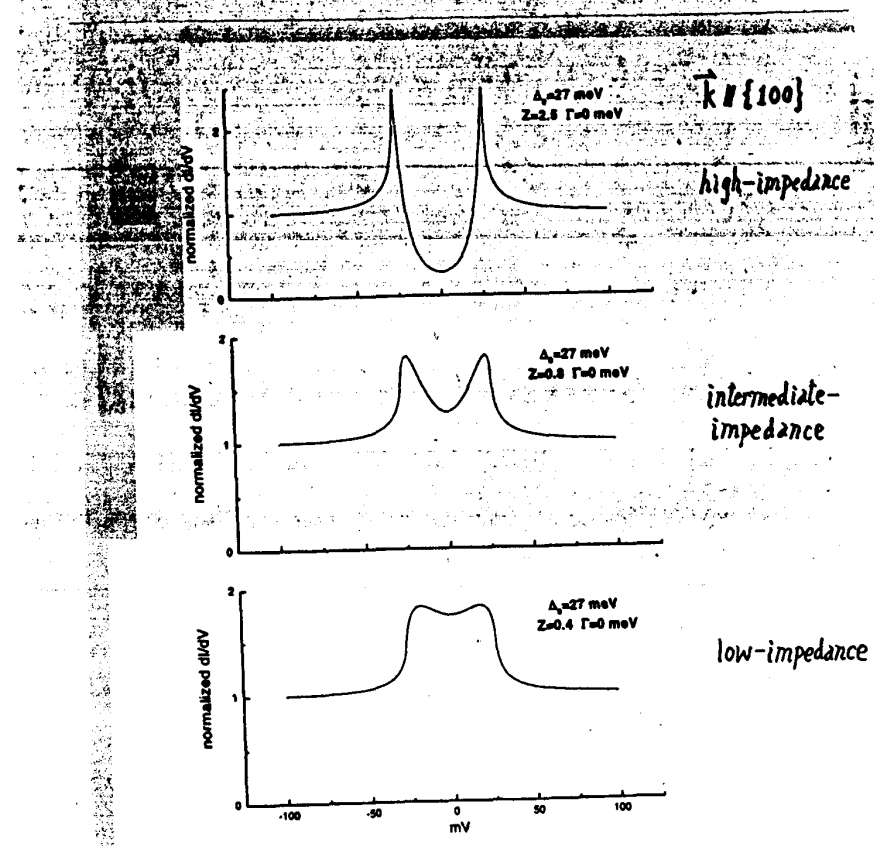
- optimally doped & underdoped $\text{YBa}_2\text{Cu}_3\text{O}_{7-\delta}$ single crystals.
- (Zn,Mg)-doped $\text{YBa}_2\text{Cu}_3\text{O}_{7-\delta}$ single crystals.
- optimally doped & underdoped $\text{La}_{2-x}\text{Sr}_x\text{CuO}_{4-\delta}$ a -axis films.

■ **Quantitative analysis:**

- the purity of $d_{x^2-y^2}$ -wave pairing symmetry.
- doping dependence of the gap Δ_d & the $(2\Delta_d/k_B T_c)$ ratio.
- comparison of STS in YBCO and in Bi-2212.
- evidence of controlled impurity scattering in $d_{x^2-y^2}$ pairing state from local density of states (LDOS).

(11)

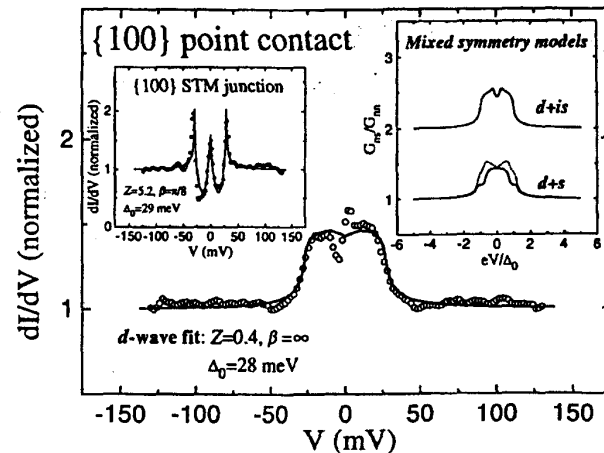
Effect of barrier strength (Z) on the in-plane {100} tunneling spectra of pure d-wave superconductors :



(12)

{100} Tunneling & Point-Contact Junctions in Optimally Doped $YBa_2Cu_3O_{7-\delta}$ Single Crystal

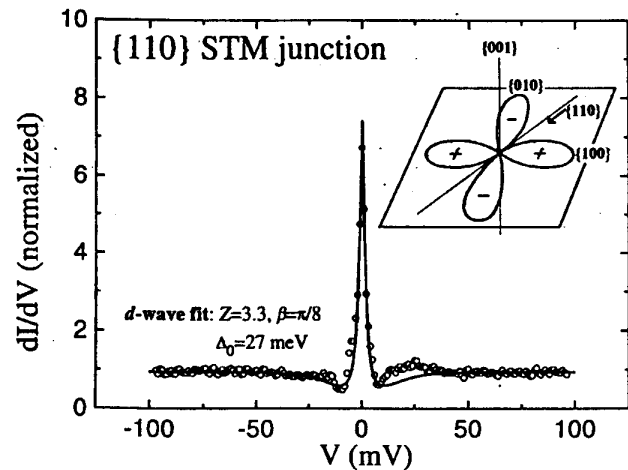
- * Low-impedance point-contact junction: Andreev reflection.
- * High-impedance tunnel junction:
superconducting gap structure & ZBCP
(any k -components different from perfect {100} contribute to ZBCP)



(13)

*{110} Tunneling Junction in Optimally Doped
 $YBa_2Cu_3O_{7-\delta}$ Single Crystal*

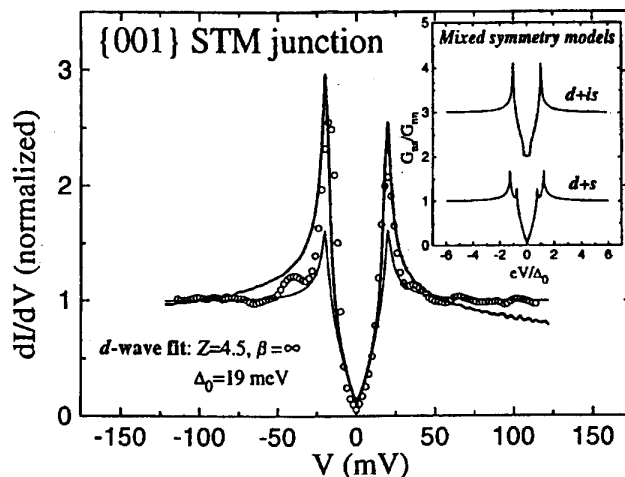
- * *No splitting in the zero-bias conductance peak (ZBCP) at $T = 4.2$ K with voltage resolution = 1 meV.*
- => *upper bound for a secondary pairing component < 5%.*



(14)

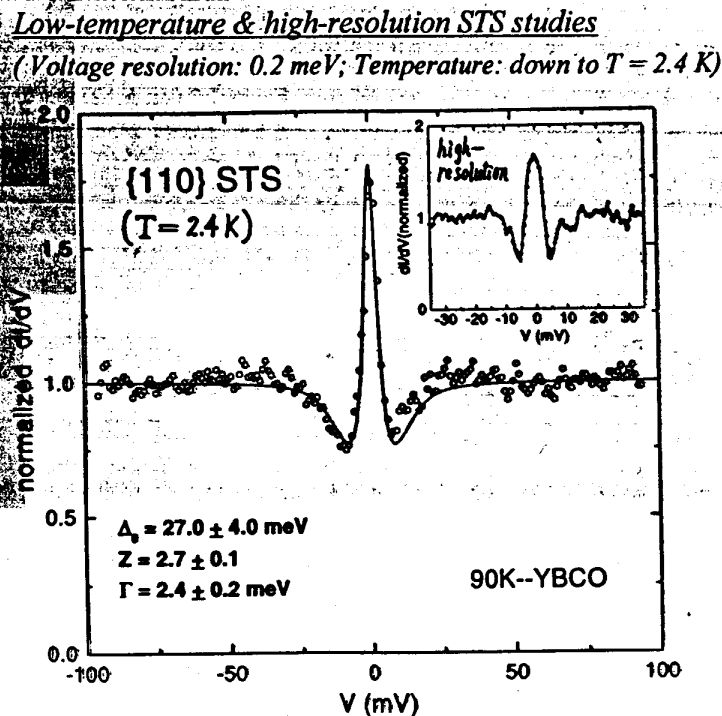
*{001} C-Axis Tunnel Junction in Optimally Doped
 $YBa_2Cu_3O_{7-\delta}$ Single Crystal*

- ◆ *Theoretical fitting incorporates two-dimensional band structures & pure $d_{x^2-y^2}$ superconducting gap:*



15

*Scanning Tunneling Spectra of Optimally Doped
 $YBa_2Cu_3O_{7-\delta}$ Single Crystal ($T_c = 91$ K)*



* No splitting in the ZBCP within our experimental resolution.

* Temperature smearing \sim voltage resolution.

16

Quality spectra allow quantitative BTK analysis :

Sample	T_c (K)	Δ_d (meV)	$(2\Delta_d/k_B T_d)$	Z
90K-YBCO{100}	91+1	29+3	7.5+0.8	5.2+0.5
90K-YBCO{110}	91+1	27+4	7.2+0.8	2.7+0.1
90K-YBCO{001}	91+1	19+4	4.9+1.0	4.5+0.5
YBCO(Zn,Mg){001}	86+1	25+3	6.7+0.8	5.0+0.5
60K-YBCO{110}	60+4	22+5	8.5+1.9	3.6+0.2
60K-YBCO{001}	60+4	17+1	6.6+0.3	4.0+0.5
LSCO ($x=0.15$) {110}	28+5	15+4	12.4+3.3	1.1+0.2
LSCO ($x=0.125$) {110}	17+5	15+4	20.5+5.5	1.2+0.2
LSCO ($x=0.10$) {100}	10+5	13+2	30.1+4.6	>1

* Upper bound for possible $(d_{x^2-y^2} + id_{xy})$ and $(d_{x^2-y^2} + is)$:

90K-YBCO : < 5%

60K-YBCO : < 9%

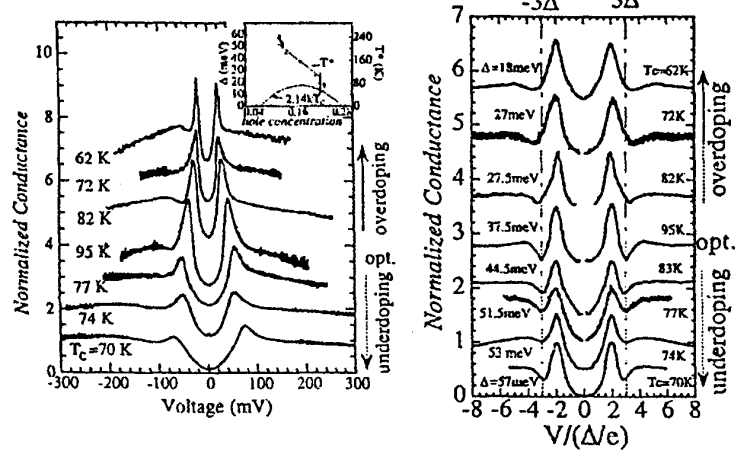
underdoped LSCO : < 9%

* Tunneling cone: $20^\circ \sim 25^\circ$

(17)

* Comparing the doping dependence of YBCO with BSCCO

(SIN & SIS c-axis point-contact data of Bi-2212)



* From N. Miyakawa et al., Phys. Rev. Lett. 83, 1018 (1999);

-- The gap feature Δ^* increases with decreasing doping level.

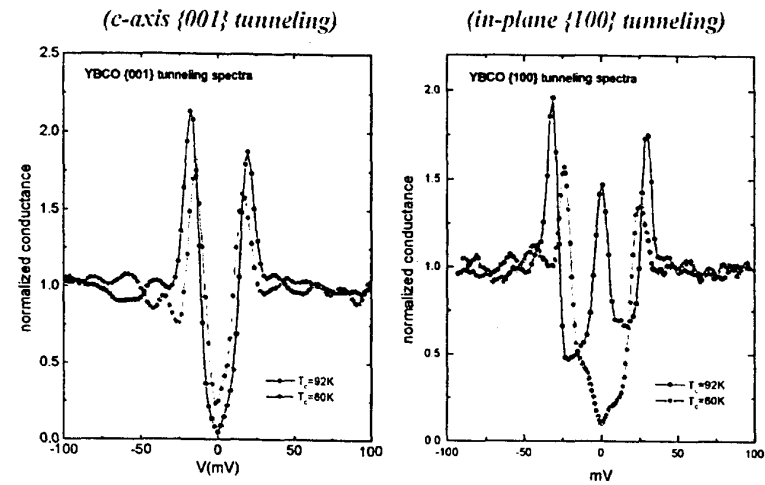
behaving like the pseudogap;

-- Additional features in the spectra:

$\Omega_{\text{dip}} \sim 2\Delta^*$ ($3\Delta^*$) and $\Omega_{\text{hump}} \sim 3\Delta^*$ ($4\Delta^*$) for SIN (SIS).

(18)

* Comparison of optimally doped & underdoped YBCO:



- With decreasing doping level:

- Δ_d decreases. \leftrightarrow decreasing superfluid density;

- $(2\Delta_d/k_B T_c)$ increases. \leftrightarrow increasing coupling.

- satellite features Ω_{dip} and Ω_{hump} scale with Δ_d :
($\Omega_{\text{dip}} \sim 2\Delta_d$ and $\Omega_{\text{hump}} \sim 3\Delta_d$).

- the relative intensity of satellite features increases.

- The satellite features are associated with the many-body effects of quasiparticle interaction with the background spin fluctuations.

- \leftrightarrow increasing importance of spin fluctuations in underdoped samples.

(19)

Comparison of YBCO & Bi-2212 :

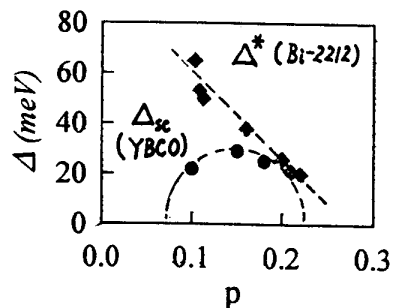
Sample	Technique	p	Δ_d (meV)	$(2\Delta_d/k_B T_c)^{**}$
YBCO(Zn,Mg){001}	STM	~ 0.18	25±3	6.7±0.8
90K-YBCO{100}	STM	~ 0.15	27±4	7.2±0.8
60K-YBCO{110}	STM	~ 0.10	22±5	8.5±1.9
Sample	Technique	p	Δ^* (meV)	$(2\Delta^*/k_B T_c)$
$\text{Bi}_2\text{Sr}_2\text{CaCu}_2\text{O}_{8+x}$	SIN & SIS	~ 0.22	~ 20	~ 6.6
	SIN & SIS	~ 0.16	~ 38	~ 6.6
	SIN & SIS	~ 0.10	~ 65	~ 6.6

** Mean-field for pure $d_{x^2-y^2}$ pairing: $(2\Delta_d/k_B T_c) = 4.28$

N. Miyakawa et al., Phys. Rev. Lett. 83, 1018 (1999).

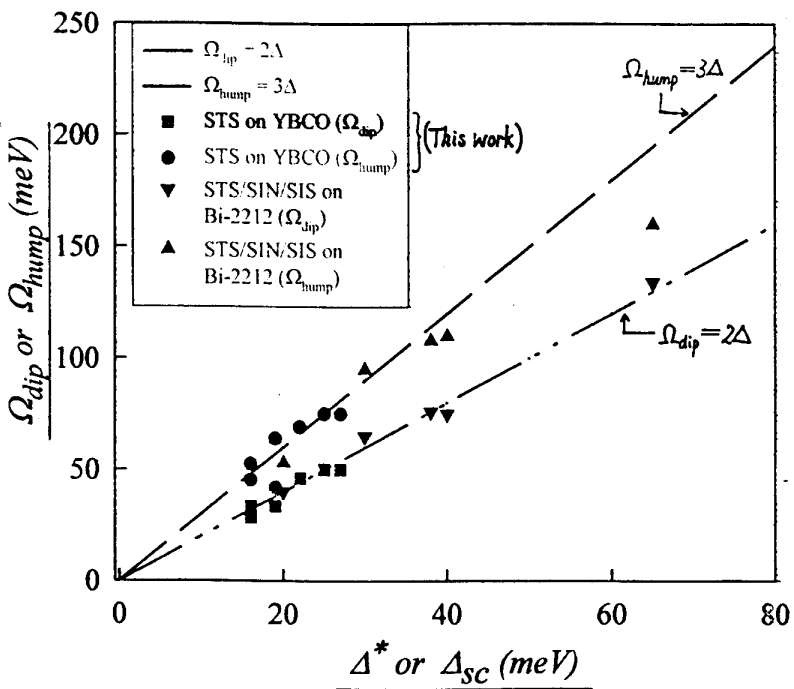
From ARPES & Knight shift data.

- Bi-2212: $\Omega_{dip} \sim 2\Delta^*$ ($3\Delta^*$) and $\Omega_{hump} \sim 3\Delta^*$ ($4\Delta^*$) from SIN (SIS);
- YBCO: $\Omega_{dip} \sim 2\Delta_d$ and $\Omega_{hump} \sim 3\Delta_d$ from STS.



(20)

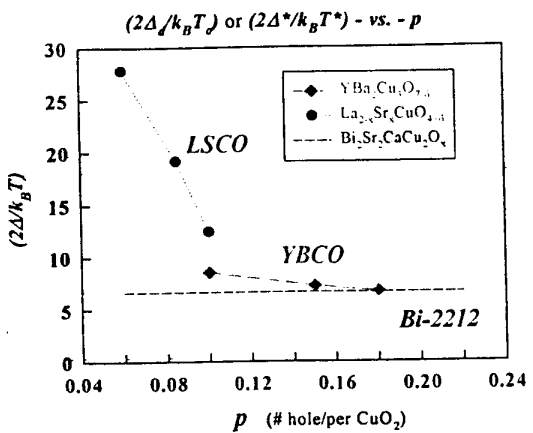
Ω_{dip} & Ω_{hump} vs. Δ_{SC} in YBCO and Δ^* in Bi-2212



Bi-2212 data: N. Miyakawa et al., PRL 83, (1999);
and Ch. Renner and O Fisher, PRB 51, (1995).

(21)

Comparing $(2\Delta/k_B T_c)$ ratio in $YBa_2Cu_3O_{7+\delta}$ & $La_{2-x}Sr_xCuO_4$ with $(2\Delta^/k_B T^*)$ ratio in $Bi_2Sr_2CaCu_2O_{8+x}$*

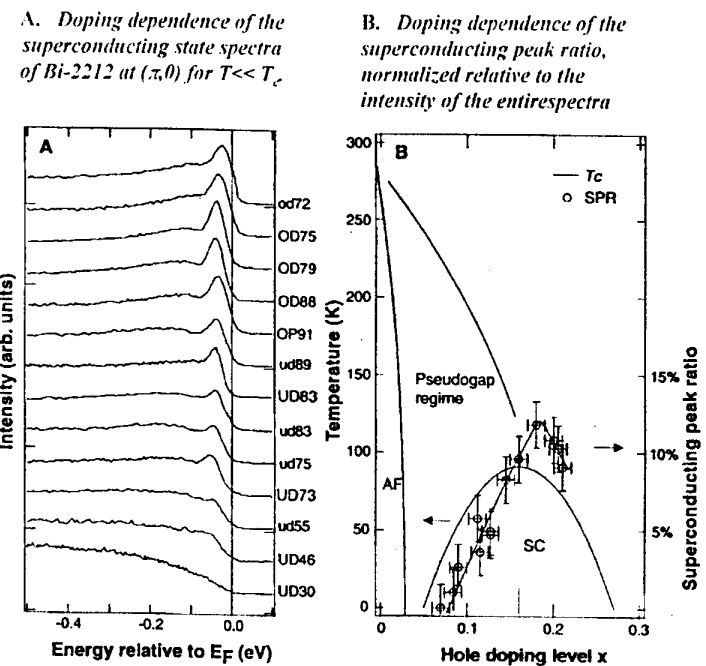


- ◆ Increasing $(2\Delta/k_B T_c)$ ratio with decreasing doping.
→ stronger coupling in underdoped samples.
- ◆ Δ^* in $Bi_2Sr_2CaCu_2O_{8+x}$ does not vanish at T_c
- ◆ T^* : the pseudogap temperature.
- ◆ On the other hand, the doping dependence of the normalized superconducting peak intensity from ARPES scales with T_c !

(22)

Signature of Superfluid Density in the Single Particle Excitation Spectrum of $Bi_2Sr_2CaCu_2O_{8+\delta}$

(D. L. Feng et al., submitted to Science)

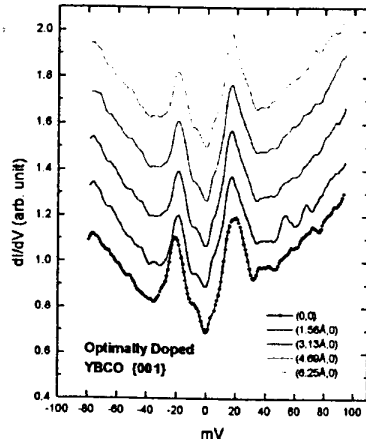


(23)

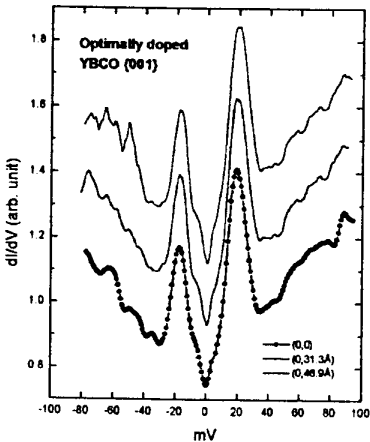
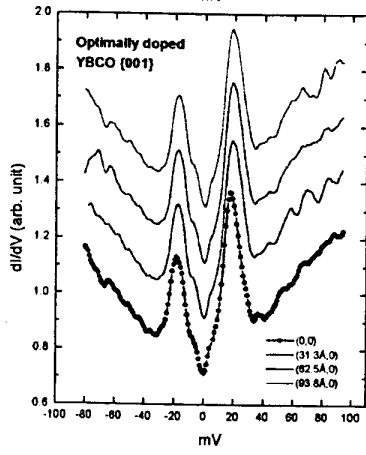
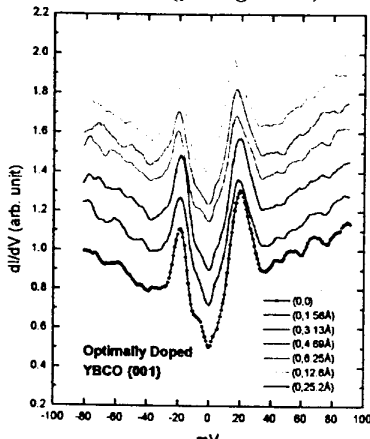
* Spatially resolved STS of pure YBCO:

- *c*-axis STS of optimally doped YBCO

(scanning along *a*-axis)



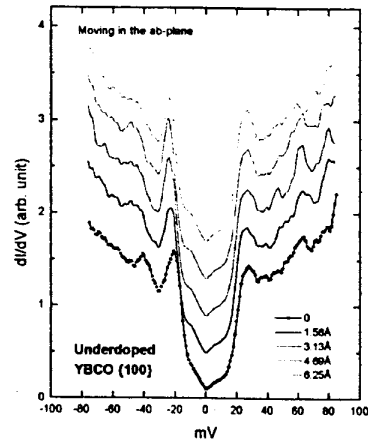
(scanning along *b*-axis)



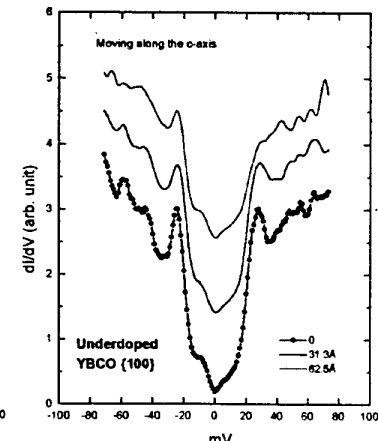
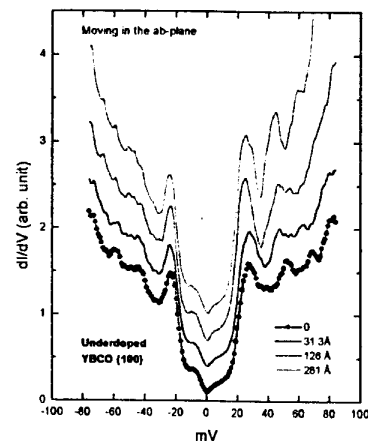
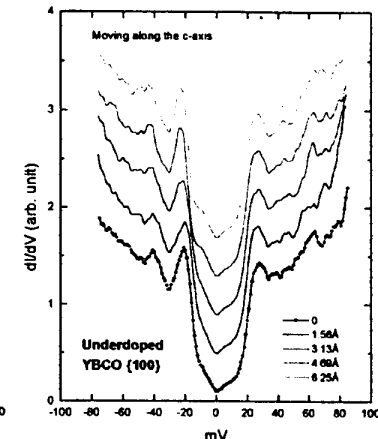
(24)

- {100} STS of underdoped YBCO:

(scanning along *b*-axis)



(scanning along *c*-axis)



(25)

* Summary of spatially STS of pure YBCO:

- For a narrow k -distribution of quasiparticles, Δ_d is spatially homogeneous over a macroscopic scale (~ 100 nm).
- The satellite features exhibit more sensitive c -axis spatial modulation.

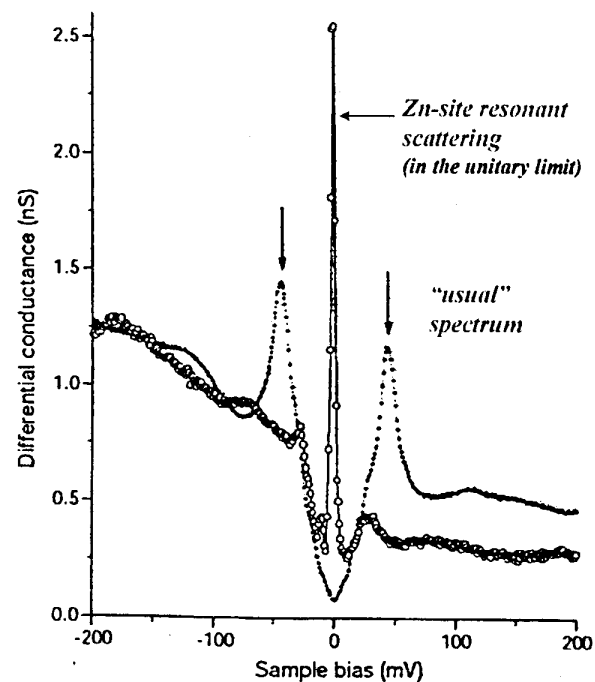
→ STS of YBCO is insensitive to weak disorder & impurities.

- What about strong pair-breakers, such as Zn substitution?

(26)

C-axis Tunneling Conductance Spectra on 0.6% Zn-doped $Bi_2Sr_2CaCu_2O_{8+\delta}$ [S. H. Pan et al., Nature 403 (2000)]

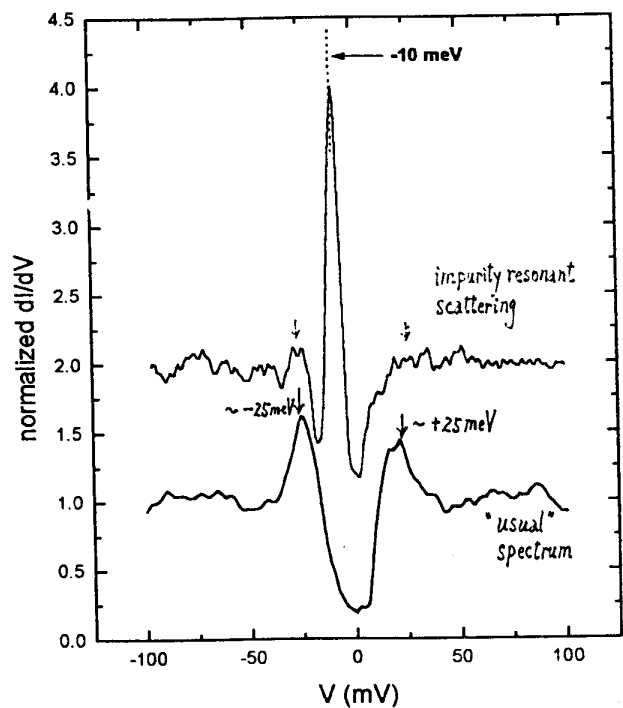
- Comparison of the local differential conductance in the "usual" superconducting region (filled circles) and at the Zn impurity site (open circles). Resonant scattering peak $\Omega = -1.5$ meV.



(27)

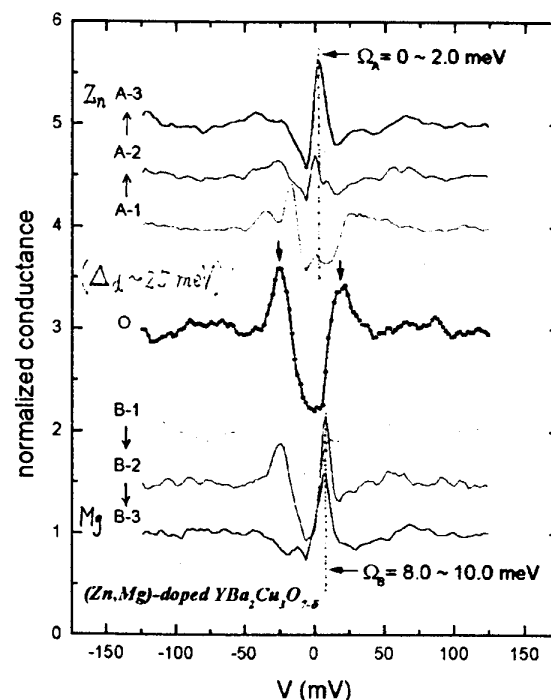
C-axis Tunneling Spectra of (Zn,Mg)-doped $YBa_2Cu_3O_{7-\delta}$
 $(Zn = 0.26\%, Mg = 0.4\%)$ [N.-C. Yeh et al., (2000)]

- ◆ Comparison of the local density of states in the “usual” superconducting region & that at an impurity site with a resonant scattering energy $\Omega_B \sim -10$ meV.



(28)

Spatial evolution of c-axis tunneling spectra of (Zn,Mg)-doped $YBa_2Cu_3O_{7-\delta}$



(29)

(30)

Scanning Tunneling Spectroscopy Studies of Non-Magnetic Impurity Scattering in (Zn,Mg)-doped $YBa_2Cu_3O_{7-\delta}$

- ◆ **Zn²⁺ replaces Cu²⁺ in the CuO₂ planes, and is known to incur strong pair-breaking effects in cuprates.**
(0.26% Zn is equivalent to 0.4% substitution of Cu in CuO₂ planes).
=> Unitary-limit resonant scattering.
- ◆ **The Mg substitution site in $YBa_2Cu_3O_{7-\delta}$ is not established;**
 - * If Mg²⁺ replaces Cu²⁺ in the CuO₂ planes,
=> weak scattering center with weak pair-breaking effects.
 - * If Mg²⁺ replaces Y³⁺,
=> overdoping YBCO, positively charged impurity site.
- ◆ **Single resonant peak at an non-magnetic impurity site,**
=> essentially pure $d_{x^2-y^2}$ pairing symmetry in YBCO.

Our STS results are consistent with the following studies:

- * **Scanning-SQUID measurements on YBCO tri-crystals:**
 - Predominant $d_{x^2-y^2}$ symmetry (> 95%) from 0.5 K to 90 K.
[Kirtley et al., *Science* **285** (1999)]
- * **Grain-boundary junctions:**
 - No splitting in ZBCP for H up to 12 Tesla and T down to 0.1 K.
[Alff et al., *Phys. Rev. B* **58** (1998); *Phys. Rev. B* **55** (1997)]
- * **STS on oriented YBCO {110} films:**
 - ZBCP becomes sharper with decreasing T.
 - No splitting in ZBCP for H up to 7 Tesla and T down to 80 mK, implying < 0.1% secondary components.
[Kashiwaya et al., *to appear in Physica C*, (2000)]
- * **C-axis STS on 0.6% Zn-substituted Bi-2212 single crystal:**
 - Single resonant scattering energy $\Omega_0 \sim - 1.5$ meV at the Zn site.
[Pan et al., *Nature* **403**, (2000)]
 - In contrast to the predictions for either $(d_{x^2-y^2} + id_{xy})$ or $(d_{x^2-y^2} + is)$ pairing. [Salkola & Schrieffer, *Phys. Rev. B* **58**, (1998)]
- * **Point-contact junctions of optimally & underdoped YBCO:**
 - [Deutscher et al., *to appear in Physica C*, (2000)]

(31)

3. Spin-Polarized Quasiparticle Transport

■ Motivation :

- * *Injection of spin-polarized quasiparticles into cuprates allows studies of:*
 - spin transport & spin-charge separation in the cuprates;
 - nonequilibrium superconductivity in d-wave superconductors.

■ Important Issues :

- * *Microscopic origin for the suppression of superconductivity by spin-polarized quasiparticles?*
 - Relevance of paramagnetic effect due to excess spins?
 - Effects of excess quasiparticles?
 - Phase decoherence due to excess spins?
- * *Characteristic length & time scales of spin transport in cuprate superconductors.*

■ Experimental Techniques :

- Critical current density (J_c) measurements.
- Scanning tunneling spectroscopy (STS).

(32)

A. Magnetic Pair Breaking Effects in Superconductors:

- * *Magnetic impurities are known to degrade superconductivity due to time-reversal symmetry breaking.*
(Ibrikosov & Gor'kov, 1961; Maki, 1963)
- * *What about spin-polarized quasiparticle currents?*
 - Excess magnetic moments:
 - paramagnetic effect;
 - magnetic exchange interaction.
 - Nonequilibrium effects:
 - redistribution of quasiparticles;
 - modification of effective temperature & chemical potential.

(33)

B. Conventional Nonequilibrium Superconductivity

■ Injection of charged quasiparticles with energy E_k

- $E_k > \Delta$: quasiparticle lifetime over time τ_{Q^*} & length l_{Q^*}
- $E_k < \Delta$: normal & Andreev reflection

(Δ : energy gap of an s-wave superconductor)

- ↔ nonequilibrium energy (T^*): the even (energy) mode
branch imbalance (Q^*): the odd (charge) mode
(Charge neutrality provided by the BCS condensate.)

$$(\delta T^*/T) = (T^* - T)/T \sim \sum_k (\delta f_k/E_k)/\mathcal{N}_0$$

$$Q^* = \sum_k f_k q_k = \sum_k f_k (\xi_k/E_k)$$

$$\delta f_k = f_k - f_k^0(E_k/k_B T), \quad E_k = (\Delta_k^2 + \xi_k^2)^{1/2} : qp \text{ energy}, \\ f_k^0(E_k/k_B T) = 1/[1 + \exp(E_k/k_B T)],$$

: equilibrium quasiparticle distribution function,

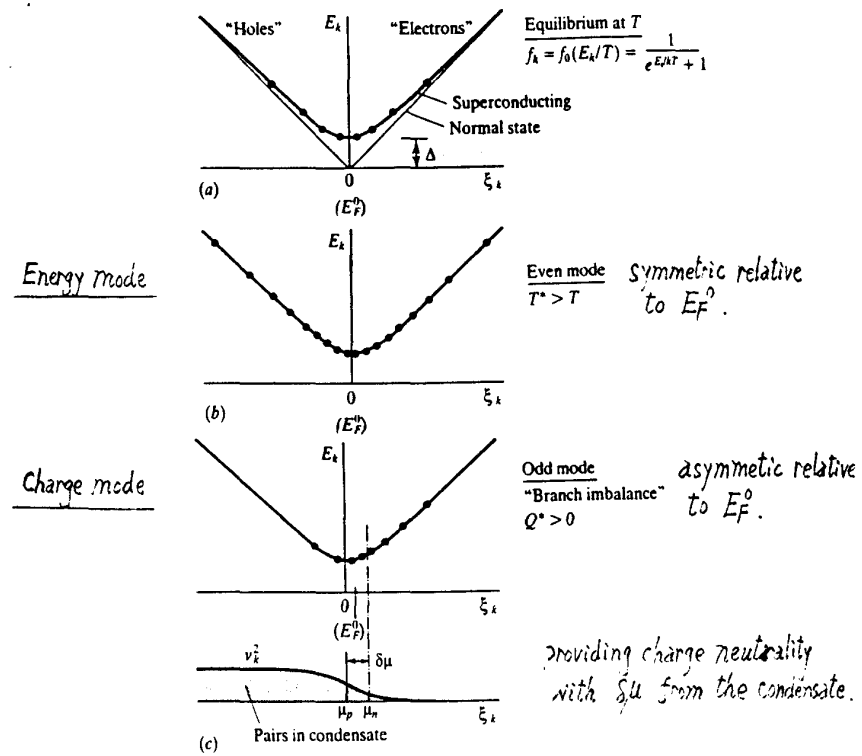
ξ_k : normal-state energy relative to E_F .

- Relaxation of non-equilibrium energy or charge:
via inelastic phonon scattering & emission near T_c ;
or elastic impurity scattering if $T \sim 0$ & anisotropic gap.

$$\tau_{T^*} \sim 3.7 \tau_E k_B T_c / \Delta(T). \quad (\tau_E \sim e\text{-ph inelastic scattering time})$$

$$\tau_{Q^*} \sim (4\pi) \tau_E k_B T_c / \Delta(T), \leftrightarrow \tau_{T^*} \& \tau_{Q^*} \text{ both diverges at } T_c$$

- Quasiparticle energy: $E_k = \sqrt{\Delta_k^2 + \xi_k^2}$. (ξ_k : single-particle energy in the normal state.)
- Probability of quasiparticle occupied state: f_k ,
(= $f_0(E_k/T)$ if thermal equilibrium)
- BCS gap equation: $\Delta_k = \sum_{k'} V_{kk'} \Delta_{k'} (1 - 2f_k)/(2E_k)$.



(34)

(35)

(36)

■ Injection of spin-polarized quasiparticles

- $E_k > \Delta$: quasiparticle lifetime over time τ_s & length l_s
- $E_k < \Delta$: no effect due to complete normal reflection
(Andreev reflection is forbidden.)
- Relaxation of spin polarized quasiparticles:
via spin-orbit scattering or magnetic exchange interaction:
 - $(\tau_s \gg \tau_{Q^*})$ & $(l_s \gg l_{Q^*})$
 - More significant pair-breaking effect of spin-polarized quasiparticles.
- * Question: How is τ_s determined microscopically?
Pair-breaking or phase decoherence
due to spin injection?
- ↔ Fermions (spin-polarized quasiparticles) interacting with Bosons (Cooper pairs).

■ Microwave-induced quasiparticles:

- Redistribution of quasiparticle (qp) DOS provided that the inelastic electron-phonon scattering time is longer than the microwave cycle.
↔ Enhancement or degradation of superconductivity.
- Departure of qp distribution (f_k) from thermal equilibrium:

$$\delta f_k = f_k - f_k^0(E_k/k_B T), \quad E_k = (\Delta_k^2 + \xi_k^2)^{1/2},$$

$$f_k^0(E_k/k_B T) = 1/[1 + \exp(E_k/k_B T)],$$

$$f_k^0: \text{equilibrium qp distribution function}$$

$$E_k: \text{qp energy} \quad \xi_k: \text{normal-state energy relative to } E_F.$$
- Effective temperature shift (δT^*) due to δf_k :

$$(\delta T^*/T) = (T^* - T)/T \sim \sum_k (\delta f_k E_k)/N_0$$

$$N_0: \text{normal-state density of states at the Fermi level}$$
- ↔ The sign of δT^* depends on that of δf_k .

(37)

Representative References:

1. "Non-equilibrium Superconductivity, Phonons, and Kapitza Boundaries", NATO ASI Series, Plenum, New York (1981), K. E. Grey (ed.), and references therein.
2. J. Clarke, *Phys. Rev. Lett.* **28**, 1363 (1972).
3. M. Tinkham and J. Clarke, *Phys. Rev. Lett.* **28**, 1366 (1972).
4. M. Tinkham, *Phys. Rev. B* **6**, 1747 (1972).
5. A. Schmid and G. Schon, *J. Low Temp. Phys.* **20**, 207 (1975).
6. G. M. Eliashberg, *JETP Lett.* **11**, 114 (1970); *Sov. Phys. JETP* **34**, 668 (1972).
7. B. I. Ivlev et al., *JETP Lett.* **13**, 333 (1971); B. I. Ivlev et al., *J. Low Temp. Phys.* **10**, 449 (1973).
8. T. M. Klapwijk and J. E. Mooij, *Physica B* **81**, 132 (1976).
9. T. M. Klapwijk, J. N. van den Berg, and J. E. Mooij, *J. Low Temp. Phys.* **26**, 385 (1977).
10. A. Schmid, *Phys. Kond. Mat.* **8**, 129 (1968).

(38)

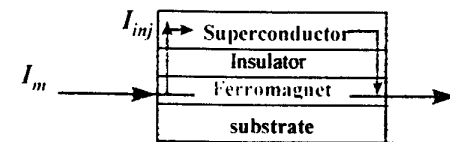
C. Suppression of High-Temperature Superconductivity by Spin Injection

■ Technical Approach:

-- Fabrication of perovskite ferromagnet-insulator-superconductor (F-I-S) heterostructures:

-- Generate spin-polarized qp's by passing electrical currents through ferromagnetic manganites, which are half-metals with nearly 100% spin polarization.

(F: CMR manganites; S: superconducting cuprates.)



* Nearly perfect lattice match of the heterostructures:

→ Epitaxial growth of the F-I-S heterostructures, preventing interface magnetic scattering.

* Predominantly d-wave pairing symmetry in HTSC

→ Directional spin-injection & low-energy qp excitations.

Current Research Status of Spin-Injection in High-Temperature Superconductors

◆ Experimental

- * V. A. Vas'ko et al., PRL 78, (1997); APL 73, (1998).
- Report suppression of critical currents (J_c) & suppression of Andreev reflection in cuprate superconductors via spin injection.
- * Z. W. Dong et al., APL 71, (1997).
- Report suppression of J_c in perovskite F-I-S.
- * N.-C. Yeh et al., PRB 60, (1999) & Physica B (2000);
J. Y. T. Wei et al., JAP 85 (1999).
- Report initial slight increase & then sharp drop in J_c upon spin-injection, using pulsed current technique to minimize Joule heating.
- Provide microscopic evidence of dynamic pair breaking based on STS.

◆ Theoretical

- * Spin-polarized quasiparticle transport & spectroscopy at various interfaces of ferromagnet & d-wave superconductor:
- Zhu, Friedman and Ting, PRB 59, (1999).
- Kashiwaya et al., PRB 60, (1999).
- Zutic and Valls, PRB 60, (1999).
- * Probing spin-charge separation, characteristic times, lengths:
- Si, PRL 78, (1997); PRL 81 (1998).
- Merrill and Si, PRL 83, (1999).

Experimental

◆ Perovskite F-I-S heterostructures:

- Ferromagnet (F): $La_{0.7}Ca_{0.3}MnO_3$ (LCMO) &
 $La_{0.7}Sr_{0.3}MnO_3$ (LSMO)
- Insulating barrier (I): YSZ or $SrTiO_3$ (STO)
- Superconductor (S): $YBa_2Cu_3O_7$ (YBCO)
- Substrate: $LaAlO_3$ (LAO)

◆ Perovskite N-I-S heterostructures (control samples):

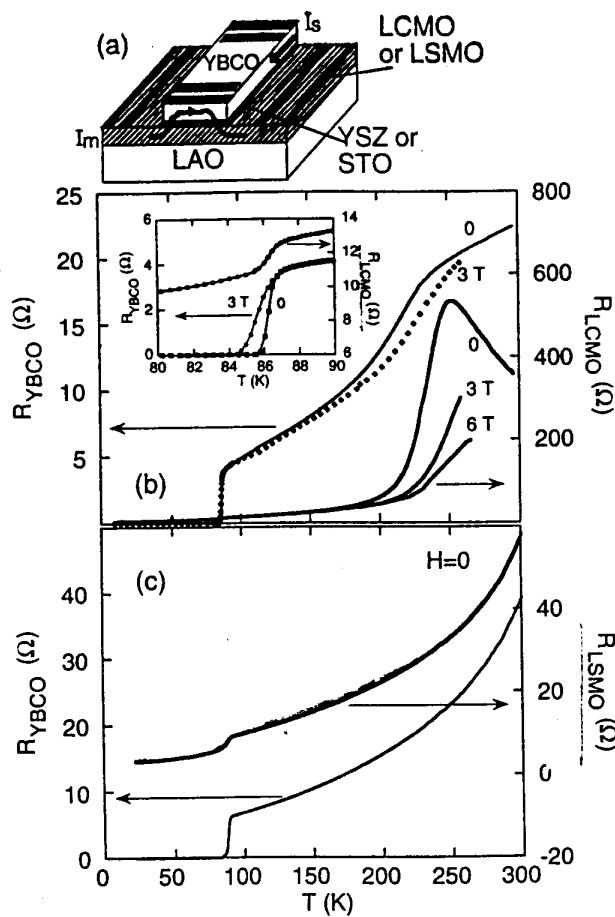
- Non-magnetic metal: $LaNiO_3$ (LNO)
- Insulating barrier: YSZ or $SrTiO_3$ (STO)
- Superconductor: $YBa_2Cu_3O_7$ (YBCO)
- Substrate: $LaAlO_3$ (LAO)

(*Pulsed laser deposition for epitaxial-film fabrication.)

◆ Measurement Techniques:

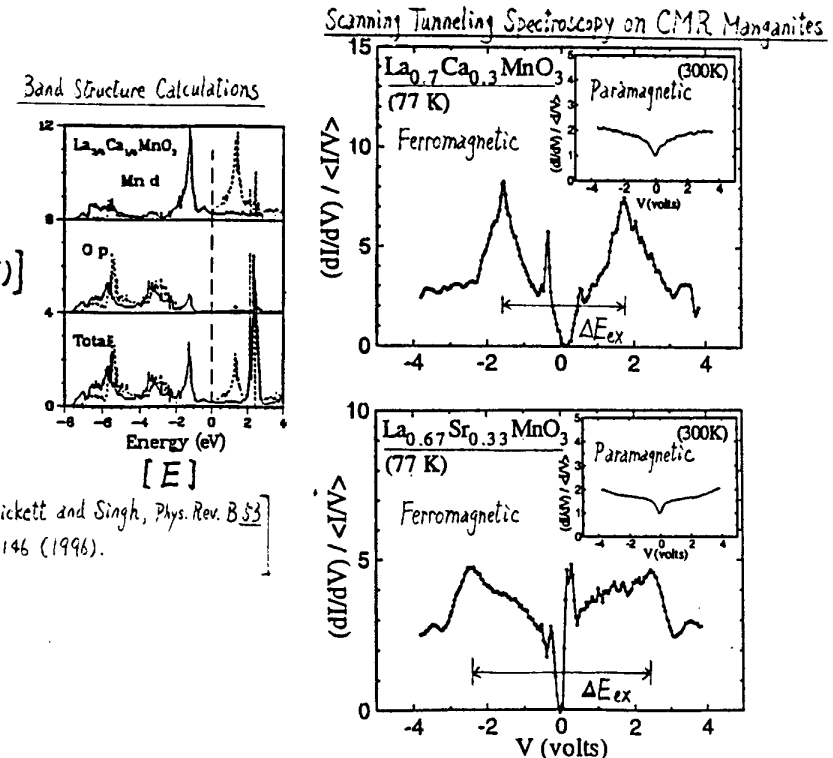
- Electrical transport: pulsed-current measurements of J_c .
- Scanning tunneling spectroscopy: quasiparticle DOS.

(41)



- $YBa_2Cu_3O_7$: $\rho_n(T_c) = 60 \mu\Omega \text{ cm}$; $T_c = 89 \text{ K}$.
- $La_{0.7}Ca_{0.3}MnO_3$: $\rho_n(300 \text{ K}) = 15 \text{ m}\Omega \text{ cm}$; $T_{\text{Curie}} = 260 \text{ K}$.
- $La_{0.7}Sr_{0.3}MnO_3$: $\rho_n(300 \text{ K}) = 2 \text{ m}\Omega \text{ cm}$; $T_{\text{Curie}} = 320 \text{ K}$.
- Interface Resistance: 0.1Ω .

- Direct evidence of half-metallic ferromagnetism in CMR manganites: [Wei, Yeh and Vasquez, Phys. Rev. Lett. 79, 5152 (1997).] [J. Appl. Phys. 83, 1997 (1998)]



Material	$T_{\text{Curie}} (\text{K})$	ΔE_{ex}
$La_{0.7}Ca_{0.3}MnO_3$	260	3.3 ± 0.2
$La_{0.7}Sr_{0.3}MnO_3$	320	4.0 ± 0.2
$La_{2/3}Sr_{1/3}MnO_3$	360	5.0 ± 0.2

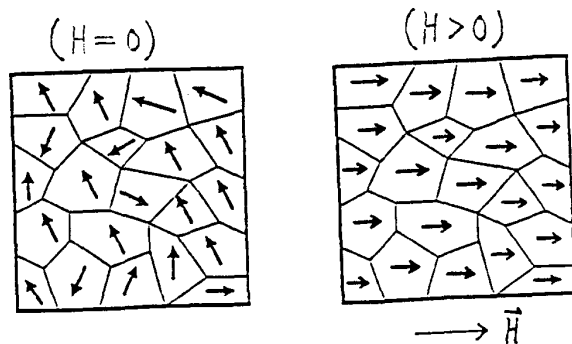
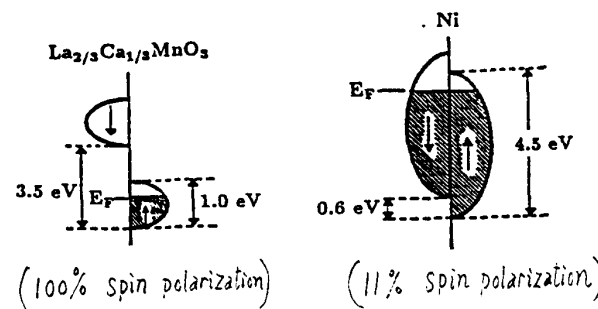
⇒ Knowledge of material properties and techniques to produce quality ferromagnetic films.

(45)

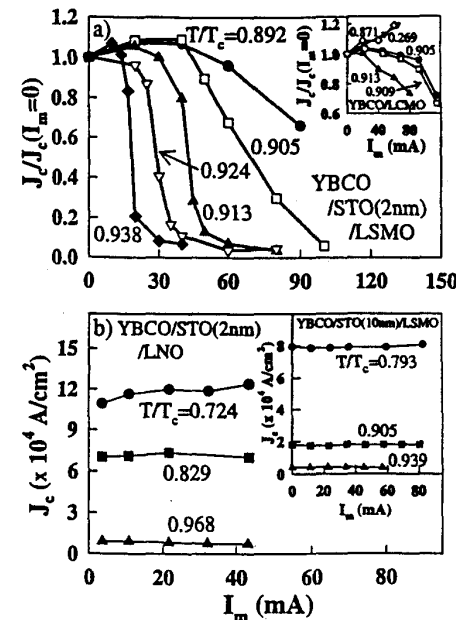
Tunneling Evidence of Half-Metallicity in Manganites

Double-exchange interaction \oplus lattice distortion

- ⇒ Half-metallicity & complete spin polarization;
 - ⇒ Colossal negative magnetoresistance. (CMR).



Effects of simple and spin-polarized quasiparticle injection current (I_m) on the J_c in N-I-S and F-I-S

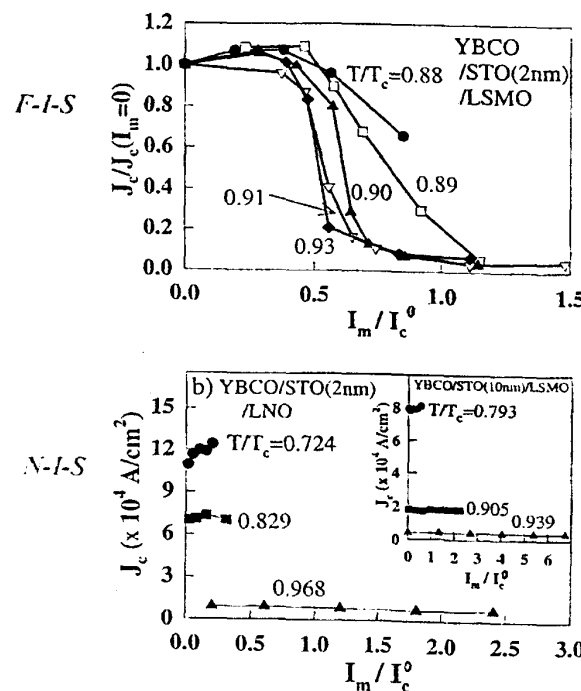


* Strong dependence of J_c on I_m in E-J-S with thin insulating barrier.

* No suppression of J_c with increasing L_m in N-I-S and in F-I-S with thick barrier.

*Comparison of Normalized Spin-Injection Effect
on F-I-S & N-I-S Heterostructures*

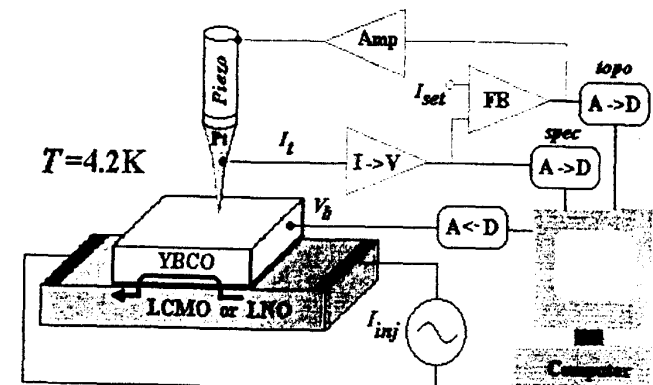
- Normalized critical current $J_c/J_c^0(T)$ vs. normalized injection current $I_m/I_c^0(T)$:



→ lifetime of spin-polarized qp (τ_s) → lifetime of simple qp (τ)

*Microscopic Evidence of Pair-Breaking
induced by Spin-Polarized Quasiparticles*

Experimental Setup :

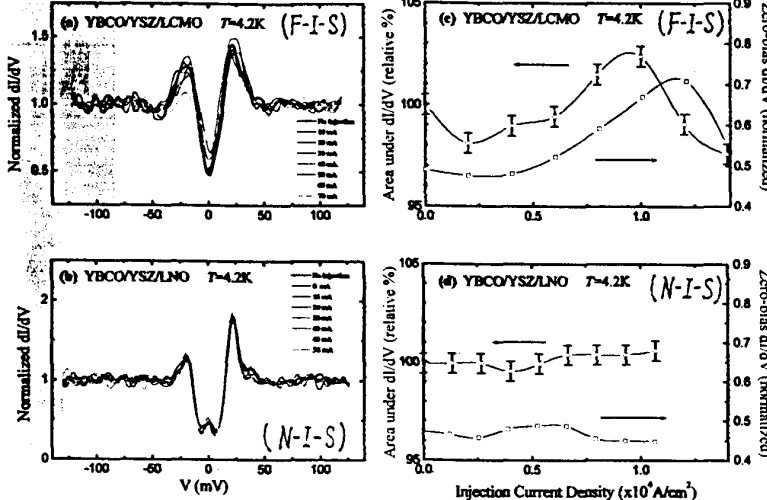


* Differential conductance (dI/dV) ~ quasiparticle density of states (dN/dE).

* Bias voltage (V) ~ quasiparticle energy (E).

(47)

Scanning Tunneling Spectroscopy of F-I-S and N-I-S Systems



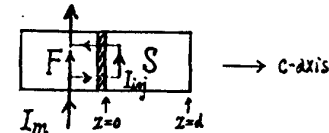
* Three major effects associated with spin-polarized currents:

- {<1> Increasing quasiparticle density of states;
- {<2> Broadening coherence peaks;
- {<3> Shifts in the chemical potential.}

(48)

Physical Concepts

♦ System of Investigation :



* Steady-state excess spin moments $m(z)$ in superconductor satisfies the diffusion equation & boundary conditions:

$$D_s \delta^2 m / \delta z^2 = m / T_f \quad T_f: \text{longitudinal spin relaxation time}$$

$$(T_f^{-1} = \lambda_{so}^{-2} \tau_{tr,spin}, \lambda_{so} \sim 0.1: \text{spin-orbit coupling})$$

$$D_s (\partial m / \partial z)_{z=0} = I_{\text{spin}} \quad D_s: \text{diffusion coefficient}$$

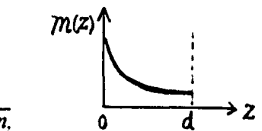
$$D_s (\partial m / \partial z)_{z=d} = 0 \quad I_{\text{spin}} = (\mu_B e) I_{\text{inj}} \quad (d: \text{thickness of YBCO})$$

$$(I_{\text{inj}}: \text{injected spin-polarized current})$$

$$(\delta_s)^2 = D_s T_f \quad (\delta_s: \text{spin-diffusion length})$$

$$\Rightarrow \text{solution: } m(z) = \{ T_f I_{\text{inj}} (\mu_B/e) / [\delta_s \sinh(d/\delta_s)] \} \cosh[(d-z)/\delta_s]$$

$$\text{average spin moments: } \bar{m} = (T_f/d) I_{\text{inj}} (\mu_B/e)$$



♦ Experimental implications :

If pair-breaking efficiency (η) is proportional to \bar{m} ,

⇒ pairing breaking effect may be enhanced by

-- increasing spin-polarized injection current I_{inj} ;

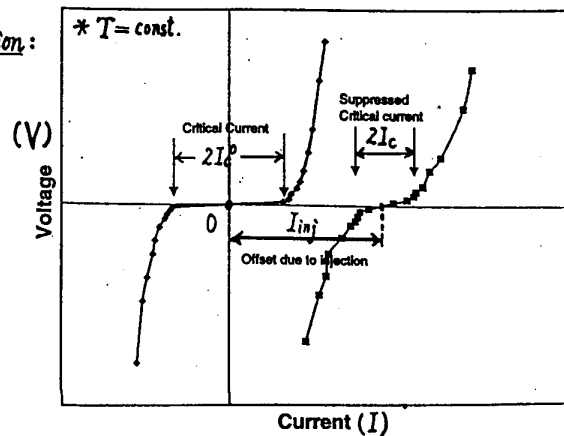
-- decreasing superconductor thickness d .

◆ Determining the efficiency (η) of pair-breaking:

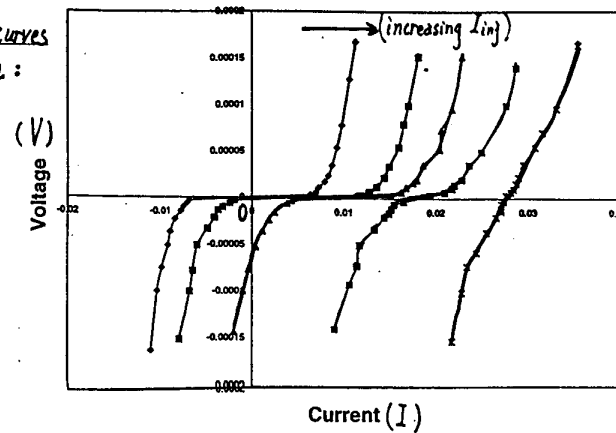
$$\eta = \Delta I_c / I_{inj} \quad (I_c: \text{critical current}, I_{inj}: \text{spin-polarized current in S.})$$

$$(\Delta I_c = I_c^0 - I_c)$$

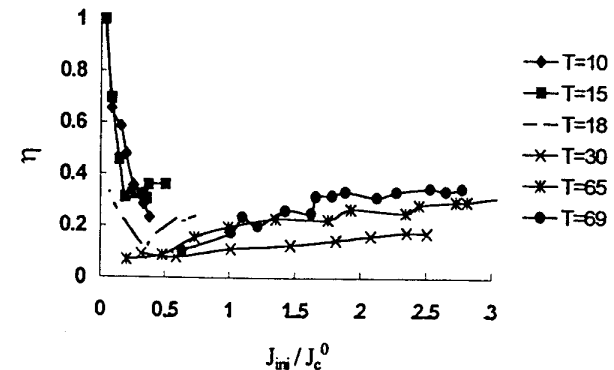
Effect of injection:



Shift of I-V curves under injection:



Temperature-dependent efficiency (η) vs. normalized injection current density (J_{inj}/J_c^0)



$$\eta \sim \langle m \rangle \sum_k (1 - 2f_k);$$

$$\langle m \rangle \sim T_1 I_{inj}/d;$$

→ relevance of quasiparticle re-distribution
(nonequilibrium effect)

(51)

Improvements to Theory

- Diffusion equation insufficient - Must consider non-equilibrium effects

- Equilibrium fermi function f_k^0 :
$$\frac{1}{1 + \exp\left[\frac{E_k}{k_b T}\right]}$$

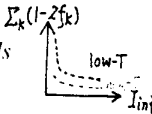
- Define new pair-breaking efficiency η : $\eta \propto \bar{m} \sum_k (1 - 2f_k)$
(Empirically, $\eta = \Delta J_c^0 / J_{\text{inj}}$)

- Under quasiparticle injection, there is a net change in chemical potential μ :
(non-equilibrium quasiparticle distribution function $f_k(I_{\text{inj}}, T)$)

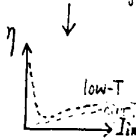
- Initially μ rises rapidly with increasing number of injected quasiparticles, and thus η drops rapidly at low T . $\mu(I_{\text{inj}})$:

- At small T , $f_k \propto \exp\left[-\frac{E_k - \mu}{k_b T}\right] \Rightarrow (1 - 2f_k)$ drops exponentially.

But eventually at high injections the chemical potential μ levels off and the efficiency η is then determined by \bar{m} . (Remember that m is proportional to the I_{inj})



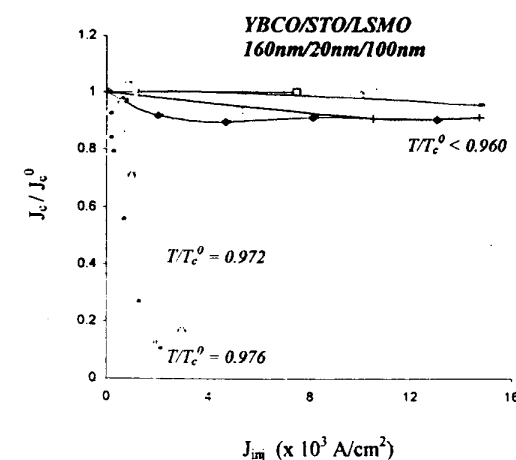
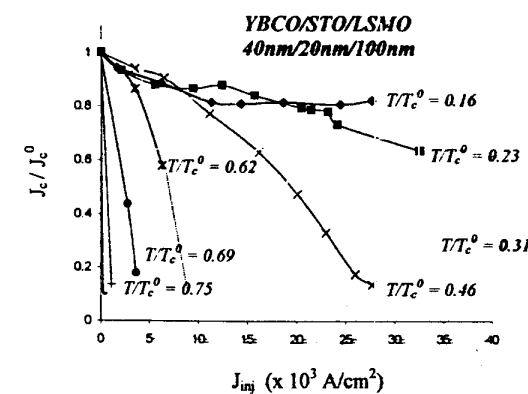
- At high T , the effect of increasing μ is diminished and η is dominated by \bar{m} .



The cross-over temperature where η becomes mostly dependent on μ gives an estimate of μ : $\mu \sim 35 k_B$

Spin-injection dependence on the superconductor thickness

(52)



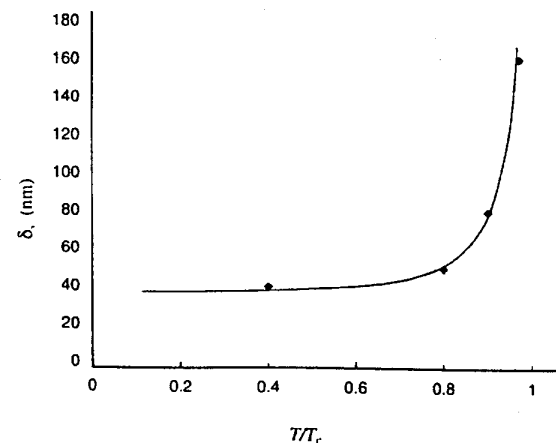
E. Implications of the Microscopic Mechanism for the Suppression of Superconductivity by Spin Injection

- ◆ Empirical estimate for the effective magnetic field:

$$B_{\text{eff}} = \mu_0 m / \Omega \sim 10^2 \text{ Tesla} \ll H_{\text{cl}} \quad (\Omega: \text{superconductor volume})$$

\leftrightarrow irrelevance of paramagnetic effect.

- ◆ Empirical estimate for the spin diffusion length $\delta_s(T)$:



→ Strong divergence of δ_s near T_c implies the relevance of spin-polarized quasiparticles to the loss of superconducting phase coherence.

Summary

- Directional & spatial resolved tunneling spectroscopy on cuprate superconductors → predominant $d_{x^2-y^2}$ pairing in:
 - optimally doped & underdoped $YBa_2Cu_3O_{7-\delta}$ (> 95%)
 - underdoped $La_{2-x}Sr_xCuO_{4-\delta}$ (> 90 %)
 - Zn-doped YBCO (> 95%).
- Comparison of YBCO & Bi-2212 tunneling spectroscopy:
 - * STS on YBCO: (maximum superconducting gap Δ_d)
 - Δ_d scales with T_c ;
 - satellite features scale with Δ_d ;
 - $(2\Delta_d/k_B T_d)$ increases with decreasing x ;
 - * STS, SIN & SIS on Bi-2212: (c-axis gap Δ^*)
 - Δ^* scales with the pseudogap T^* ;
 - $(2\Delta^*/k_B T^*) \sim 6.6$ for all x ;
 - * ARPES on Bi-2212: ($\pi, 0$) superconducting peak
 - the relative intensity scales with T_c
 - \leftrightarrow Relevance of the doping level & spin fluctuations to the pairing state and symmetry of high-temperature superconductivity.

◆ *Spin-injection studies in $YBa_2Cu_3O_{7-\delta}$:*

* *Evidence of nonequilibrium quasiparticle redistribution*

-- increasing suppression of superconductivity with

- 1) increasing spin injection (I_{inj});
- 2) decreasing superconductor thickness (d).

* *The c-axis spin diffusion length (δ_s):*

1) increases rapidly near T_c ;

2) $\delta_s \sim 50$ nm for $T \ll T_c$ & 100 nm $< \delta_s < 200$ nm for $T \sim 0.9 T_c$

* *Negligible paramagnetic effect due to injected spins.*

↔ “dephasing” (rather than pair breaking) effect of
spin-polarized quasiparticles on Cooper pairs.